ISSN 1590-8844
International Journal of Mechanics and Control, Vol. 18, No. 02, 2017

DESIGN OPTIMIZATION OF A SAFETY CLAMP FOR PORTABLE MEDICAL DEVICES

P. Boscariol* G. Boschetti* R. Caracciolo* M. Neri*/** D. Richiedei* C. Ronco** A. Trevisani*

*Department of Management and Engineering, Università degli Studi di Padova, Vicenza, Italy

**Department of Nephrology, Dialysis and Transplantation, S. Bortolo Hospital, Vicenza, Italy

ABSTRACT

Portable kidney replacement systems and ultrafiltration devices can be used to treat patients with renal deficiencies. Such devices work by filtering the blood directly taken from patients and by reinfusing it after the purification. This procedure must be performed under strict safety conditions, which include the use of a safety clamp capable of stopping the external body blood circulation in case of a safety hazard, such as the formation of clots, air bubbles and blood backflow. The model-based design of a novel electromechanical clamp is presented in this paper, since the commercially available ones cannot comply with the strict requirements in terms of size, weight and power consumption imposed by the portability of the ultrafiltration device under investigation. The clamp is based on an articulated mechanism, whose dimensions are optimized to achieve adequate clamping force and low power consumption.

Keywords: Clamping device, Wearable Ultrafiltration System, Design optimization, Miniaturized mechanism

1 INTRODUCTION

Patients suffering from chronic kidney disease often require to be treated with support therapies which involve blood purification. Blood purification can be performed by passing the blood, taken from a vascular access, through a semipermeable membrane, which can reduce the solutes and the water, thus supporting the reduced functionality of the kidneys. After purification, blood is reinfused into patients [1,2]. This procedure is commonly performed by special-purpose machines in hospitals, where patients can find also trained personnel and medical supervision. However, such treatments represent a heavy burden for patients, which usually must visit hospitals at least three times a week for several hours. Such inconvenience can be reduced by performing similar treatments with minimum interference to patients' life [3]. Additionally, a reduced hospital stay would provide a clear economic advantage for national health services [4].

Contact author: Alberto Trevisani

Stradella S. Nicola 3, 36100 Vicenza, Italy
E-mail: alberto.trevisani@unipd.it

These considerations have fostered the developments of portable renal replacement devices, often referred to as Wearable Artificial Kidneys (WAK) and Wearable Ultra Filtration Systems (WUF). Some of such devices have reached an advanced development phase and are currently in clinical trial phase [2]. However, because of the complexity of the design and the several critical issues imposed by the application field, no commercially available solutions have been developed yet. This fact combined with the existence of still open and relevant research issues, justifies further research effort in this field. A major limitation to the diffusion of wearable/portable ultrafiltration devices is the concurrent need for miniaturization, safety and reduced power consumption. The conditions under which such devices must work, i.e. connected with the patient's circulatory system, impose strict safety requirements and a thorough risk management analysis. Any portable device must drain and reinfuse blood from patients, who are therefore exposed to the risk of blood clots, blood losses, blood reverse flow and injection of air bubbles into the venous circulation systems. Any of these occurrences should trigger an alarm and an immediate occlusion of the extracorporeal blood circulation. The non-portable devices used in hospitals perform this operation using an automatic pinch valve, often referred to as "clamp". Clamps work by mechanically occluding the tube which carries the patient's blood, thus isolating the patient from a malfunctioning device.

While several components of the ultrafiltration device are disposable, namely the one that are in contact with the patient's blood, a clamp is usually non-disposable and therefore operates by pinching the tube. Maximum safety and capability of operating under a power supply failure impose the definition of a normally closed operation, as in the case of commercially available pinch valves [5,6]. Such devices are however unsuitable for a portable, battery-operated device. Being conceived for non-portable applications, they result in being too bulky and non-sufficiently energy efficient for the application under consideration in this work. A major concern posed by traditional clamping systems is the high temperature of operation, induced by the large and continuous power consumption, typically larger than 10 W. The high temperature of a component can be a serious problem in the design of a portable device.

A novel clamp design is investigated in this paper, by proposing an articulated mechanism, whose dimensions are optimized to meet the strict requirements imposed by the application. Primary design goals include limited space occupation, adequate force exerting capability and reduced power consumption. A normally closed operation must be ensured as well, as previously explained.

To the best of Authors' knowledge, the literature does not provide solutions which are compliant, at the same time, with all such strict design requirements. The commercially available solutions are for the vast majority based on the use of a voice-coil actuator with a linear spring, in which the latter is used to ensure normally-closed operation. As already stated, their power consumption is by far unsuitable for the wearable device under development. Other solutions have been developed for industrial applications, in which clamps are often used to hold a workpiece. The popularity of the application has fostered a fluent literature on the mechanical design of such devices [7], that are in their most common implementation, either hand-operated or hydraulic operated linkages. By carefully tuning the dimension of an articulated mechanism, a sufficient force advantage, i.e. a ratio between the produced force and the actuation force, can be obtained. A further investigation on the same topic [8] also include the analysis and the optimization of a clamping mechanism by taking into consideration not only the static force distribution, but also the elastic displacements produced by the forces acting on the mechanism. Similar concepts can be applied to the current study, if energy efficiency and smallest power and force requirements are included in the design specifications. The choice of the mechanisms that are usually employed for industrial applications, which usually use linear hydraulic actuators [9], are unsuitable for the application under development here. Preliminary design considerations have excluded the possibility of using linear actuators, and batteries are the only power source allowed in practice for this kind of application. Moreover, off-the-shelf industrial clamps do not exert clamping force in case of a power source failure, as it is strictly required in the case of the safety device under consideration in this work.

Hence, a novel design based on cascaded four-bar linkages, is proposed in this paper. The design is optimized to achieve adequate force amplification to work with a small-size stepper motor. Normally closed operation is ensured by checking the dynamic behaviour of the mechanism when the electric motor is turned off.

2 DESIGN SPECIFICATIONS

All the design specifications to be met by the clamp must ensure the essential goal of achieving maximum safety to avoid any possible hazardous situation. The correct operation of the device is the normally closed one. This feature is commonly achieved using a spring preload, which can be counteracted by an electric actuator. Since the clamp should not get in contact with blood, the flow is regulated by pinching the tube into which blood flows. The analysis of the commercially available solutions has highlighted that a clamp to be used with 4.2 mm-diameter PVC tube requires at least 4.2 W to keep blood flowing. Such a power consumption is unsuitable for a wearable battery-operated device. Indeed, an ultrafiltration treatment usually lasts up to 24 hours, thus a 100 Wh battery capacity would be required just to power the safety clamp. This power capacity implies using batteries weighting between 500 g and 1 kg, according to the average power density of off-the-shelf lithium-ion batteries [11]. Both the weight and the generated heat are too high to provide a comfortable solution. To reduce both the battery weight and heat generation, the maximum power consumption is imposed to be lower than 1 W as a design specification to be met in this work. Preliminary tests have shown that the chosen 4.2 mm-diameter tube requires a maximum pinch force approximately equal to 25 N in the typical range of tube materials and dimensions. By choosing a safety factor equal to 2, the force that need to be exerted by the clamp should be at least equal to 50 N. This choice might allow adapting the clamp to a configuration in which both the inlet and outlet tubes need to be pinched by a single device.

The clamping force should be provided by the spring preload alone, since the desired tube occlusion should be performed without the aid of the actuator. Such a force must be provided for a clamp displacement that is at least equal to the size of the internal tube diameter, which is 2.6 mm in the system under investigation. If a maximum blood flow equal to 70 ml/min is considered [12], then the linear speed of the blood is equal to 0.224 m/s. Thus, blood flow should be stopped within 0.67 s if the distance between the last safety sensor and the patient's vascular access is at least equal to 150 mm, as chosen in the layout of the system. Finally, if a safety factor of 10 is used in this situation to improve safety, the design target is to ensure a complete occlusion with 67 ms from the detection of the fault.

The clamp design, developed in accordance with the specifications, is introduced in the next section and its performance are discussed. A preliminary design is presented, together with the procedure used to obtain an optimized one.

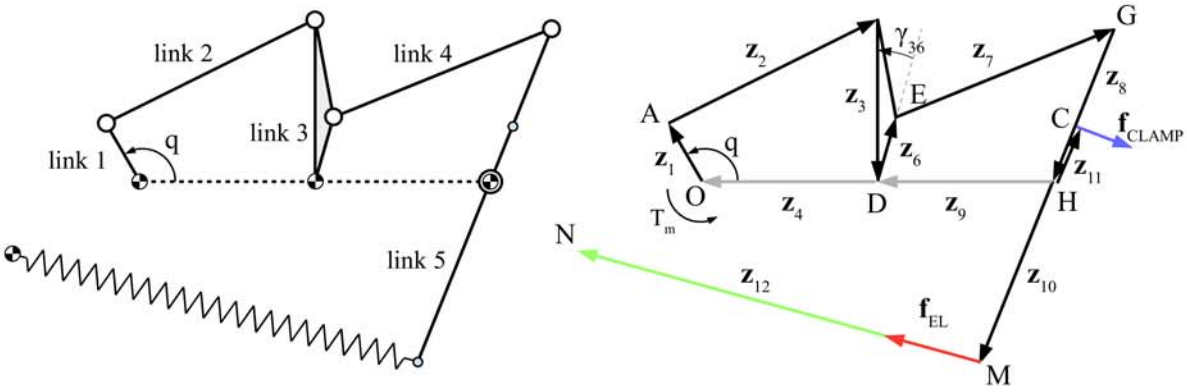

Figure 1 Clamp: kinematic scheme and external forces exerted on the mechanism

3 MECHANICAL DESIGN

The design of the clamp is based on a multi-loop articulated mechanism. According to the kinematic scheme in Fig. 1, the mechanism is defined as the cascade of two four-bar linkages. The coupling between the two four-bar mechanisms is provided by the ternary link 3. The choice of an articulated design is motivated by the need to achieve high force advantage, thus requiring a reduced size actuator. A careful design of articulated mechanisms, moreover, allows to reduce to a minimum the overall size of the device. The preliminary CAD design, shown in Fig. 2, shows that the mechanism can be fit almost entirely within the footprint of the actuator. The design avoids the use of prismatic joints to comply with the manufacturing limitations imposed by the rapid-prototyping machine used to produce a working sample of the device.

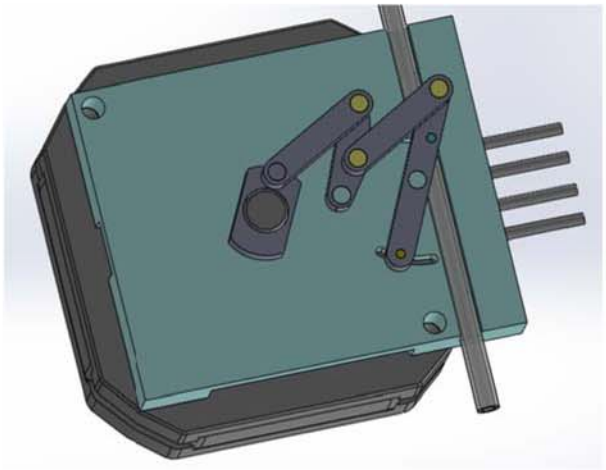

Figure 2 Clamp: preliminary CAD design, mechanism shown in closed configuration

Figure 2 shows the mechanism in the closed configuration. The spring is hosted between the ground link (shown in light blue) and the electric motor. According to the kinematic scheme of Fig. 1, the motor provides torque T_m about joint O and drives link 1 directly.

No reduction gear has been introduced in the design to reduce the number of elements of the mechanism and to ensure backdrivability of the mechanism. Backdrivability is essential for the correct operation of the device and is the capability of the force exerted by the spring to overcome the motor detent torque and the resistant force opposed by the tube and promptly move the mechanism in case of need. The fixed end of the spring is located at point N, while the other end is connected to link 5 at point M. The choice of the spring ad its location must ensure a adequate magnitude of the force f_{CLAMP} exerted on the tube where blood flows. Tube pinching is provided by a small size metal pin located at point C on link 5. Spring preload is, during normal operation, counteracted by the counter-clockwise torque exerted by the motor, which is amplified by the closed kinematic chain. According to the main design goals stated in section 2, the design of the mechanism must be optimized to accomplish a minimization of the motor size, as well as of the overall size of the device. The design procedure has involved the definition of the length of the links, of the joint positions and of the spring parameters. The goal of the optimization is the minimization of the maximum torque that the motor should provide to open the mechanism. The motor torque, which depends on the value of the independent coordinate q, is evaluated within the usable workspace Q, which is defined as the range of the angular rotation of the driving link 1 between the open and the closed configurations. The achievement of a feasible design as the result of a numerical optimization technique is ensured by defining some constraints. The first constraint is set on the displacement of the pinching element: it must be ensured that the overall displacement of point C is adequate to produce a displacement that is at least equal to the inner diameter of the tube, i.e. 2.6 mm. Additionally, the force exerted on the tube, denoted f_{CLAMP} in Fig. 1, must be higher than 50 N. These two constraints require a careful trade-off: a larger displacement of point C is achieved by reducing the ratio between the lengths z_3 and z_1, as well as the ratio between z_8 and z_6, as well as with the increase of the length z_{11}. However, these changes in turn have the negative effect of reducing the force advantage.

The equilibrium equations for the mechanism can be inferred through the principle of virtual works in all the pinching configurations. When the motor is switched off, the sole external forces acting on the mechanism are the spring pull $\boldsymbol{f}_{EL}$ and the clamping force $\boldsymbol{f}_{CLAMP}$. The resulting static equilibrium is therefore:

$$\begin{bmatrix} f_{EL}^x & f_{EL}^y \end{bmatrix} \begin{bmatrix} \frac{\partial x_M}{\partial q} \\ \frac{\partial y_M}{\partial q} \end{bmatrix} + \begin{bmatrix} f_{CLAMP}^x & f_{CLAMP}^y \end{bmatrix} \begin{bmatrix} \frac{\partial x_C}{\partial q} \\ \frac{\partial y_C}{\partial q} \end{bmatrix} = 0 \tag{1}$$

Equation (1) includes the sensitivity coefficients of the cartesian positions of points C and H, which can be evaluated as:

$$\frac{\partial x_C}{\partial q} = z_{11} \sin(\varphi_{11}) \frac{\partial \varphi_8}{\partial q} \tag{2}$$

$$\frac{\partial y_C}{\partial q} = -z_{11} \cos(\varphi_{11}) \frac{\partial \varphi_8}{\partial q} \tag{3}$$

$$\frac{\partial x_M}{\partial q} = -z_{10} \sin(\varphi_8) \frac{\partial \varphi_8}{\partial q} \tag{4}$$

$$\frac{\partial y_M}{\partial q} = z_{10} \cos(\varphi_8) \frac{\partial \varphi_8}{\partial q} \tag{5}$$

In Eqs. (2-5), and throughout the whole paper, the angles φ_i $(i = 1, \dots, 12)$ denote the absolute angular position of vectors $\boldsymbol{z}_i$. The computation of Eq. (2-5) requires evaluating the following sensitivity coefficient:

$$\frac{\partial \varphi_8}{\partial q} = \frac{z_1 z_6}{z_3 z_8} \frac{\sin(q - \varphi_2)}{\sin(\varphi_2 - \varphi_3)} \frac{\sin(\varphi_6 - \varphi_7)}{\sin(\varphi_7 - \varphi_8)} \tag{6}$$

Equation (1) will be included in the optimization routine to ensure a sufficiently large occlusion force, thus allowing for the achievement of a proper spring design.
The actuator effort in the open configuration is evaluated by including the effects of the torque generated by the motor, T_m, and the spring pull. The small force due to the interaction with the tube in this phase is reasonably neglected. The resulting static equilibrium equation is:

$$\begin{bmatrix} f_{EL}^x & f_{EL}^y \end{bmatrix} \begin{bmatrix} \frac{\partial x_M}{\partial q} \\ \frac{\partial y_M}{\partial q} \end{bmatrix} + T_m = 0 \tag{7}$$

Although all the design parameters of the mechanism have a strong influence on its performances, the large number of variables suggests including just a subset of them within the optimization parameters vector. Indeed, the effectiveness and the convergence of a nonlinear constrained optimization routine is easily jeopardized by large scale problems [10]. Therefore, the number of optimization parameters has been kept to a minimum by performing a preliminary design of the mechanism, which has involved the choice of the lengths of the links of the two cascaded four-bar mechanisms.

Such a preliminary design has been carried out considering that the mechanical advantage is directly proportional, among the others, to the ratios of the link lengths z_3/z_1, z_6/z_8 as shown in Eq. (6), as well as the ratio z_8/z_{11}, which appear in the sensitivity coefficients of Eq. (2-5). These ratios have therefore been set to be as high as possible, considering also the trade-off between getting high force magnification and assuring an adequate displacement at point C, and while avoiding interference or collisions. The effects of the other geometrical parameters included in the design have a less straightforward interpretation and therefore their values will be defined through the numerical optimization. The numerical optimization routine therefore includes the following design parameter vector:

$$\boldsymbol{x} = [x_N, y_N, L_0, z_{10}, \gamma_{36}] \tag{8}$$

Parameters z_{10}, L_0, x_N and y_N set the design of the spring-loading mechanism to be optimized, being L_0 the free length of the spring. Moreover, the constant angle between vectors $\boldsymbol{z}_3$ and $\boldsymbol{z}_6$, denoted γ_{36}, is to be determined through the optimization routine as well. This parameter has a strong influence on the performance of the mechanism, since it affects both the absolute value of the sensitivity coefficient $\partial\varphi_8/\partial q$ and the overall displacement of the contact point C, as shown in Fig. 3 and Fig. 4.

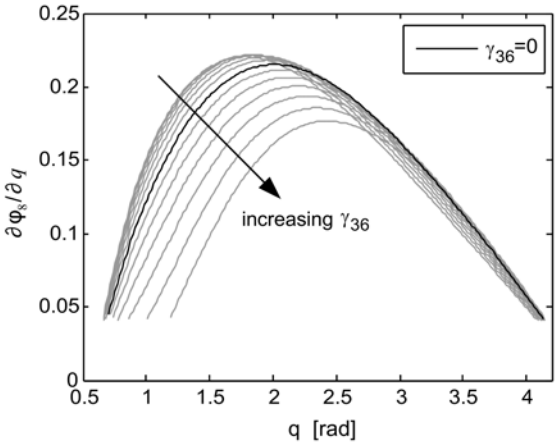

Figure 3 Sensitivity coefficient $\partial\varphi_8/\partial q$ vs q with different choices of γ_{36} in the $\pm\pi/6$ range

Figure 3 shows how $\partial\varphi_8/\partial q$ is affected by γ_{36} in the range $\pm\pi/6$ rad. Results are reported for the usable workspace Q, which is defined as the subset of the whole workspace for which $\partial\varphi_8/\partial q$ is adequately far from singularity to assure backdrivability, and that the torque needed to counteract the spring pull always takes positive values. Such a threshold has been chosen equal to 0.04. Figure 3 reveals that larger values of γ_{36} lead to higher force magnification.
Figure 4 shows the total displacement of the contact point C against γ_{36}. The results reveal that larger values of γ_{36} reduce the amplitude of the displacement of the pinching element, up to the point that the displacement of point C is too small to produce a full tube occlusion.

The most suitable value of γ_{36} must therefore result from a careful trade-off between these two opposite effects. Such a feature will be ensured through the solution of the optimization routine.

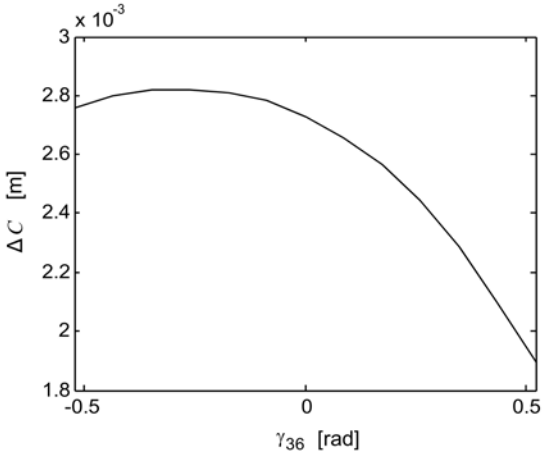

Figure 4 Maximum displacement of point C vs. γ_{36}

The stiffness of the spring has been chosen by evaluating the trade-off between the overall size and the needed stiffness, considering that the latter should provide an adequately large force with a small displacement.
The resulting optimization procedure produces an optimal choice of the five parameters included in vector $\boldsymbol{x}$ that minimizes the scalar cost function J defined as follows:

$$J = \min_{q \in Q} \max T_m(q, \boldsymbol{x}) \tag{9}$$

The cost function J of Eq. (9) is chosen to minimize the peak value of the torque that the motor must exert to counteract the spring pull throughout the whole usable workspace. Such a motor torque can be computed according to the equilibrium of Eq. (7). The choice of a "minmax" cost function is chosen to minimize the size of the motor, given the peculiar use of the clamp which consists in keeping the clamp open, i.e. with negligible exerted torque, for most of the time. Hence, the most critical motor parameter is the maximum torque.
The need for a feasible optimal design requires to include into the optimization routine some constraints, that result in nonlinear constraints:

$$f_{CLAMP} \geq 50 \text{ N} \tag{10a}$$
$$\Delta C \geq 2.6 \text{ mm} \tag{10b}$$
$$y_N \leq -5 \text{ mm} \tag{10c}$$

The first constraint ensures that the clamping force is sufficient to produce a full occlusion of the tube, and is evaluated according to Eq. (1). The constraint of Eq. (10b) is set to ensure a sufficiently large displacement of point C throughout the workspace Q. Such a displacement is set to be at least equal to the inner diameter of the tube.

The third constraint is chosen to ensure that there is no interference between the fixed end of the spring, located at point N, and the shaft of the motor.
The design optimization has been performed by using a pattern search method based on the simplex algorithm. The outcome of the minimization procedure has been compared with the result of a genetic algorithm procedure [13], which has produced the same results, thus corroborating the convergence of the optimization. The parameters of the optimized design are shown in Table 1. The table lists also the position of the fixed revolute joints, the link lengths, the spring stiffness k and the spring free length L_0.

Table I – Optimal design parameters

O = [0;0] mm	D = [8.5; 0] mm	H = [17;0] mm
N = [-14;-5] mm	z_1= 4 mm	z_2= 12 mm
z_3= 10 mm	z_6= 4 mm	z_7= 12 mm
z_8= 10 mm	z_{10}= 8.5 mm	z_{11}= 5.3 mm
γ_{36}= 0.2187 rad	k = 3000 N/m	L_0= 16 mm

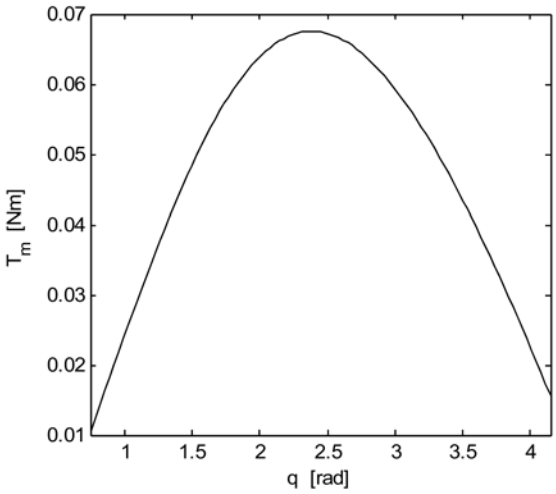

Figure 5 Motor torque T_m vs independent coordinate q

The resulting motor torque is represented in Fig. 5 for all the configurations within the usable workspace Q. The small peak torque needed to achieve the equilibrium allows for the use of a relatively small size motor with no gearboxes. The clamping force is shown in Fig. 6. It also complies with the design specifications, since it is larger than 50 N for every configuration within the usable workspace Q. The clamp is completely closed for $q = 0.7429$ rad, for which the force exerted on the tube is equal to 50 N. Such a configuration is equilibrated by a minimum value of the motor torque T_m, according to Fig. 5, since link 1 and 2 are almost aligned. The fully open configuration corresponds to $q = 4.153$ rad: in this configuration, the motor must produce a torque that is roughly equal to 0.015 Nm. Such a small value ensures a reduced power consumption in the normal operation of the device.

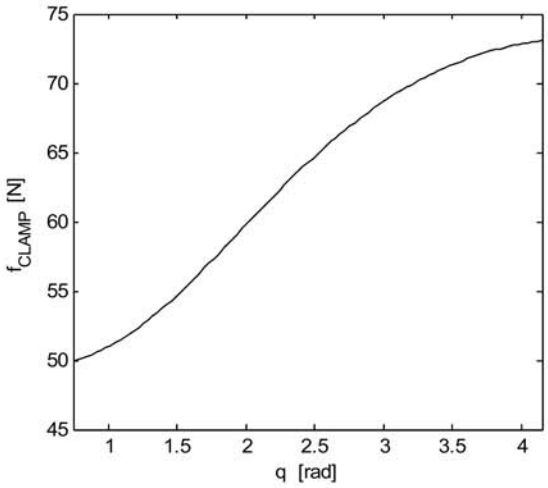

Figure 6 Clamping force f_{CLAMP} vs independent coordinate q

The position analysis of the mechanism is sketched in Fig. 7, which shows the configurations of the mechanism for ten equally spaced crank positions within the usable workspace Q. The figure shows that link 1 and 2 are close to the alignment for both the open and the closed configuration.

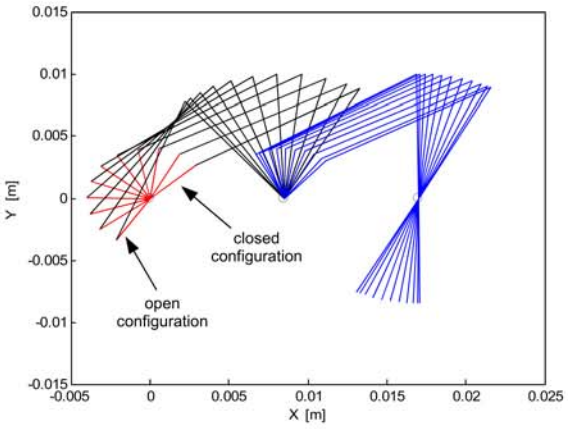

Figure 7 Mechanism displacement throughout the workspace Q

The actual displacement of the clamping point for the optimized design is shown in Fig. 8. Such a plot shows that the total displacement of the point C is equal to 2.6 mm, and is therefore adequately large to produce a full occlusion of the blood-carrying tube. This feature has been enforced by the nonlinear constraint of Eq. (10b). Given the required, a pancake Sanyo Denki stepper motor has been chosen. Such a motor can provide a continuous holding torque equal to 83 mNm when operated using 24 V DC power supply. The choice of a stepper motor is motivated by the common unavailability of slim profile DC motors. The advantages of the reduced space occupation of a stepper motor comes at the cost of a less simple drive circuit, that is required to provide the correct current at each phase of the motor.

The motor can provide the needed torque to keep the clamp in the open position with a power consumption that is estimated to be nominally equal to 143 mW (i.e. without considering the power losses of the driving circuit and the efficiency loss due to the heating of the motor). This value satisfies the design specification of 1 W.

In order to verify that the complete closure of the pipe is obtained within the required maximum time, the dynamic response of the mechanism is investigated through forward dynamic analysis. This analysis is needed to evaluate whether the system can avoid the injection of an air bubble into the patient's circulating system by occluding the pipe in a sufficiently small amount of time.

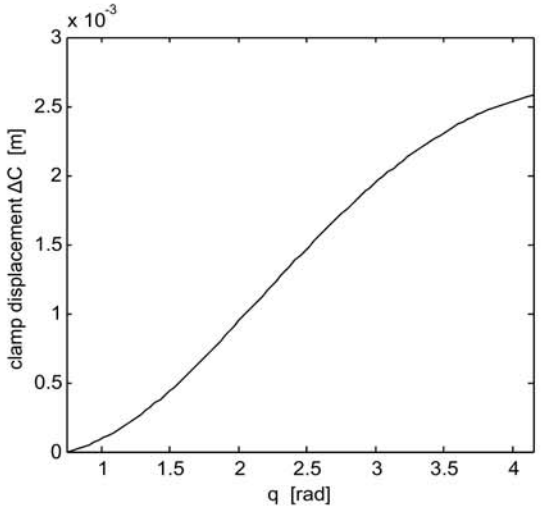

Figure 8 Clamp displacement vs independent coordinate q.

The system dynamics has been therefore modelled by accounting for the spring force, the inertial contribution of the motor shaft, and by representing the tube resistant force as a constant term $f_{tube} = 25$ N.

Additionally, the detent torque T_d (i.e. the torque required to rotate the motor shaft with no current applied to the windings) of the stepper motor has explicitly considered in the evaluation and estimated as 1/10 of the motor holding torque, as it often happens in commercial motors.

Such a value has been also experimentally verified through direct measurements on a motor sample. Other sources of friction, such as the friction at the joints, are neglected. Indeed, it is reasonable assuming that friction at the joint can be kept small by introducing suitable joint clearance.

Such a clearance does not affect significantly the motion of the mechanism, given the presence of spring preload. In order to consider a worst-case scenario, an overall constant inertia J_{tot} equal to twice the motor one has been considered (J_{tot}= $0.03 \cdot 10^{-4}$ kgm^2). The approximated dynamic model during the spring-induced motion can therefore be written as:

$$J_{tot}\ddot{q}(t) = f_{EL}^{x}\frac{\partial x_M}{\partial q} + f_{EL}^{y}\frac{\partial y_M}{\partial q} - T_d - f_{tube}\frac{\partial x_C}{\partial q} \qquad (11)$$

Equation (11) has been integrated from the initial conditions $q = 4.153$ rad and $\dot{q} = 0$ rad/s.
The solution of the forward dynamics highlights that the complete pipe obstruction, which happens when $q = 0.7429$ rad, is achieved after just 49 ms. Considering that the speed of blood along the tubes is roughly equal to 0.224 m/s and that the response time of the blood detector sensor is equal to 100 ms, air bubbles can only travel 33 mm after their detection. Therefore, to assure that air bubbles could be stopped even before reaching the clamp, a reasonable distance between the bubble detector and the clamp should be approximately 50 mm to include further safety margins.

4 CONCLUSIONS

In this paper, the model-based design of a novel clamp for portable kidney replacement systems and ultrafiltration devices is proposed. The design of this component includes the synthesis of an articulated mechanism which can be driven by a small size electric motor without the use of a gearbox. The design of the mechanism has been optimized to reduce the maximum torque the motor must exert to open the clamp, while achieving good mechanical advantage in the open position of the clamp and assuring a prompt closing of the clamp in case of emergency. The proposed design is shown to achieve very good results in terms of miniaturization and power consumption, also in comparison with commercially available clamping devices for medical use.

ACKNOWLEDGMENTS

Authors acknowledge the financial support by Fondazione Cariverona through a Ph.D. scholarship and the research grant "RAP" Ricerca Scientifica e Tecnologica 2014.

REFERENCES

[1] Drukker W, Parsons F.M. and Mahe J.F, *Replacement of renal function by dialysis: a textbook of dialysis*, Springer Science & Business Media, 2012.

[2] Davenport A., Portable and wearable dialysis devices for the treatment of patients with end-stage kidney failure: Wishful thinking or just over the horizon? *Pediatric Nephrology*, Vol. 30, pp. 2053-2060, 2015.

[3] Ronco C., Davenport A., Gura V, The future of the artificial kidney: moving towards wearable and miniaturized devices. *Nefrologia*, Vol. 31, No. 1, pp. 9-16, 2011.

[4] Gura V., Beizai M., Exon C., Rambod E., Continuous renal replacement therapy for congestive heart failure: the wearable continuous ultrafiltration system. *ASAIO Journal*, Vol. 52, No. 1, pp. 59-61, 2006.

[5] Clippard Instrument Laboratory, Inc. – USA, www.clippard.com

[6] SONCEBOZ SA - CH, www.sonceboz.com

[7] Tso P., The kinematic synthesis of toggle clamps, *Journal of Manufacturing Science and Engineering,* Vol. 120, No. 3, pp. 648-655, 1998.

[8] Ming-Shyan Huang, Tsung-Yen Lin, Rong-Fong Fung, Key Design parameters and optimal design of a five-point double-toggle clamping mechanism, *Journal of Applied Mathematical Modelling*, Vol. 35, No. 9, pp.4304-4320, 2011.

[9] Guang Ju S., Min Zhong K., Peng Jia J., Two-Point Floating Clamping Device Based on Fixed Cylinder with Double-Piston and Toggle-Lever Force Amplifier, *Advanced Materials Research*. Vol. 201. Trans Tech Publications, 2011.

[10] Rao R.V., Savsani V.J., Mechanical Design Optimization Using Advanced Optimization Techniques, Springer Series in Advanced Manufacturing, 2012.

[11] Thackeray M.M., Wolverton C., Isaacs E.D.: Electrical energy storage for transportation – approaching the limits of, and going beyond, lithium-ion batteries. *Energy & Environmental Science*, Vol. 5, No. 7, pp. 7854-7863, 2012.

[12] Boschetti G., Dalla Via A., De Rossi N., Garzotto F., Neri, M., Pamato L., Ronco C., Trevisani A., Conceptual design of a mechatronic biomedical wearable device for blood ultrafiltration, *Proc. of 1st International Conference of IFToMM ITALY, IFIT 2016*, Vicenza; Italy; 1-2 December 2016, pp. 89-96, 2016.

[13] Cabrera, J.A., Simon A, Prado M. Optimal synthesis of mechanisms with genetic algorithms. *Mechanism and Machine Theory* Vol. 37, No, pp 1165-1177, 2002.